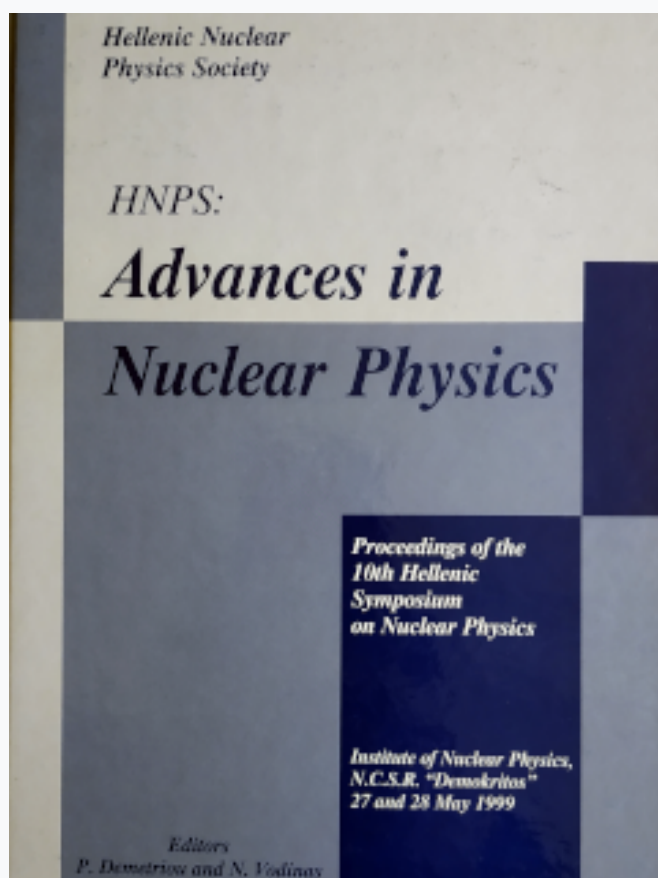


## Annual Symposium of the Hellenic Nuclear Physics Society

Τόμ. 10 (1999)

HNPS1999



### Intermediate-Energy Fragmentation of Heavy-Element Beams: A Novel Approach Towards the Nuclear Drip-Lines

G. A. Souliotis

doi: [10.12681/hnps.2188](https://doi.org/10.12681/hnps.2188)

### Βιβλιογραφική αναφορά:

Souliotis, G. A. (2019). Intermediate-Energy Fragmentation of Heavy-Element Beams: A Novel Approach Towards the Nuclear Drip-Lines. *Annual Symposium of the Hellenic Nuclear Physics Society*, 10, 179–193.  
<https://doi.org/10.12681/hnps.2188>

# Intermediate-Energy Fragmentation of Heavy-Element Beams: A Novel Approach Towards the Nuclear Drip-Lines

G. A. Souliotis <sup>1</sup>

*Institute of Nuclear Physics, NCSR Demokritos, Athens, Greece.*

---

## Abstract

The fragmentation of heavy beams at intermediate energy and the opportunities offered by this in the exploration of heavy nuclei near the drip lines will be discussed. First, a study of  $^{197}\text{Au}$  projectile fragmentation at 30 MeV/nucleon will be presented in which an appreciable number of new p-rich nuclei were observed. Perspectives of proton radioactivity studies using the fragmentation approach will be discussed. Second, a study of the fission of  $^{238}\text{U}$  projectiles at 20 MeV/nucleon will be presented, where a number of new neutron rich nuclei were identified. Production rates of extremely n-rich nuclides from a typical projectile-fragmentation facility are given. A large number of nuclei along the astrophysical r-process path can be investigated and approach of the neutron dripline in the region  $Z=45-50$  may be possible. The ability to produce and study these either p-rich or n-rich nuclei at intermediate (and possibly lower) energy facilities may open a variety of possibilities for experimental studies of exotic heavy nuclei.

---

## 1 Introduction

Access of unexplored regions of the chart of the nuclides has recently become possible by the production and use of radioactive nuclear beams (RNBs) [1]. Radioactive beams are produced by two main principles: ISOL (Isotope Separation-On-Line) and IFS (In-Flight Separation) or PF (Projectile Fragmentation) principles. ISOL techniques [2] offer very high intensity beams, but require separation times of 1–20 sec. On the other hand, IFS techniques [3] are characterized by fast separation times ( $<1\ \mu\text{sec}$ ) and rather moderate intensities, offering the possibility of accessing and studying very short lived proton-rich or neutron-rich nuclei at the limits of stability [4].

---

<sup>1</sup> e-mail address: soulioti@cyclades.nrcps.ariadne-t.gr

Fragmentation of heavy target nuclei by energetic protons has been known as an important path for the synthesis of new proton-rich nuclei. The large intensity of the proton beams, the large penetrating power (enabling the use of thick targets and high production rates) and the high excitation energies of the reaction intermediates all lead to the efficient production of proton-rich nuclei. This fact has been recognized in the design of several radioactive beam facilities which are Isotope Separation On-Line (ISOL) facilities.

Projectile fragmentation (PF) facilities, while not having the overall beam intensities of ISOL facilities, have some advantages that complement the ISOL facilities. In particular, the lack of a release or delay time in a PF facility allows the study and use of short-lived nuclides not accessible in ISOL facilities. Recently this feature has been used in relativistic[5] and intermediate energy studies[6] to produce and study several new, short-lived neutron rich nuclei.

A recent measurement of the fragment yield distributions for the reaction of 20 MeV/nucleon  $^{197}\text{Au} + ^{nat}\text{Ti}$  and  $^{90}\text{Zr}$  provided evidence for the formation of very p-rich nuclei [7]. However, the exploratory character of that study did not provide a clear identification of new p-rich species. The possibility of using intermediate-energy  $^{197}\text{Au}$  projectiles to generate and identify new proton-rich nuclides was further investigated. Specifically, the distributions of heavy residues from the interaction of 30 MeV/nucleon  $^{197}\text{Au}$  projectiles with  $^{90}\text{Zr}$  were studied using a high-resolution spectrometer/detector system. The measurements showed that new proton-rich nuclides can be identified among the reaction products of this reaction. After a short description of the experiment and analysis procedures, the mass and charge distributions of heavy residues from the Au+Zr reaction are presented. Finally, possibilities of nuclear studies of p-rich nuclei offered by the PF approach are discussed.

Concerning the generation of neutron-rich nuclei, recent work done at GSI [5] has demonstrated that a projectile fragmentation (PF) facility can be a useful source of n-rich secondary beams. These experiments, involving fission of relativistic (750 MeV/nucleon)  $^{238}\text{U}$  ions, demonstrated the production of a large number (more than 100) of new n-rich radionuclides. The production mechanism was low-energy fission induced by electromagnetic excitation and peripheral nuclear interactions [5].

In the present work, we investigated the fission of intermediate-energy  $^{238}\text{U}$  projectiles to generate and identify new neutron-rich nuclides. For this purpose, we studied the fission fragments from the interaction of 20 MeV/nucleon  $^{238}\text{U}$  projectiles with  $^{208}\text{Pb}$ . The measurements showed that very n-rich nuclides are produced in this reaction and can be unambiguously identified. Also, estimates of production cross sections and rates of new very n-rich nuclides from a typical second-generation PF facility are given.

Finally, a summary of the present work on very heavy beams at intermediate energy and the possibilities of drip-line studies are presented.

## 2 Production of Proton-Rich Nuclides by $^{197}\text{Au}$ Projectile Fragmentation

The experimental work on  $^{197}\text{Au}$  projectile fragmentation was performed at the National Superconducting Cyclotron Laboratory at Michigan State University using the A1200 fragment separator. The use of this separator as a high resolution spectrometer has been discussed previously [6,8–10]. A 30 MeV/nucleon  $^{197}\text{Au}$  beam ( $i = 0.3$  particle nA) struck a production target of  $^{90}\text{Zr}$  ( $1.0 \text{ mg/cm}^2$ ) with an inclination of  $1^\circ$  with respect to the axis of the spectrometer. Recoiling fragments from the target passed through a slit defining a 3% momentum acceptance, a position sensitive parallel plate avalanche counter (PPAC) and a thin ( $0.22 \text{ mg/cm}^2$ ) aluminum emitter foil of a microchannel plate timing system (giving a start signal) at the first dispersive focus of the spectrometer. At the focal plane of the spectrometer ( $\sim 14 \text{ m}$  from the start detector) the fragments passed through another thin ( $0.22 \text{ mg/cm}^2$ ) aluminum emitter foil of a second microchannel plate timing system (giving a stop signal) and then into a three element ( $55\mu$ ,  $50\mu$ , and  $300\mu$ ) silicon detector telescope. The minimum observed fragment flight time was  $\sim 200 \text{ ns}$ . For each event, the fragment time-of-flight,  $dE/dx$ ,  $E$  and magnetic rigidity ( $B\rho$ ) were recorded. From these quantities, the values of the atomic number  $Z$ , velocity, mass-to-charge ratio  $A/q$ , atomic charge  $q$  and mass number  $A$ , were calculated for each fragment. The spectrometer was calibrated by measuring its response to analog beams of  $^{62}\text{Ni}$ ,  $^{68}\text{Zn}$ ,  $^{124}\text{Sn}$ ,  $^{129}\text{Xe}$ ,  $^{180}\text{W}$ ,  $^{197}\text{Au}$ , and  $^{208}\text{Pb}$ . The details of the calibration procedure are discussed elsewhere[10].

Typical examples of  $Z$ ,  $q$  and  $A$  spectra of heavy fragments from this reaction at a single setting of the spectrometer are shown in Fig. 1. The values of the resolution (FWHM) associated with the measurement of these quantities are 0.9, 0.9 and 0.8, respectively, for the heavier fragments. After summing over all observed  $q$  values and velocities, the mass distributions of the various isotopes ( $Z=50-84$ ) were obtained. For a number of elements in the region  $Z=60-73$  (see Fig. 2), there is evidence for the formation of “new” proton-rich nuclei. Estimates of production cross sections are obtained as described in [10,7].

The general features of the yield distributions of the reaction products are first presented, before discussing further on the new p-rich nuclei. In Fig 3, the velocity integrated yield distributions are shown as  $Z$ - $A$  contour plots with the  $Z$  coordinate given relative to the line of  $\beta$  stability [11]. The average fragment  $Z$ - $A$  values expected from relativistic nuclear collisions (dashed line) [12], the so-called “evaporation residue attractor line” (EAL)[13] (dash-dotted line), and the position of the proton-drip line for odd- $Z$  nuclei [14,15] (solid line) are shown in the figure. [ The EAL is a line in the  $N$ - $Z$  plane that represents the locus of fragment yields produced by the evaporation of neutrons and charged particles from highly excited nuclei.] One does note that the reaction products are very proton-rich, some having 7 or more protons than the stable isobar. The centroids of the yields are more p-rich than those obtained in relativistic nuclear collisions, and seem to follow the evaporation residue attractor line rather closely. Interestingly, a substantial fraction of the yields lie at and beyond the position of the proton dripline. Detailed fragment

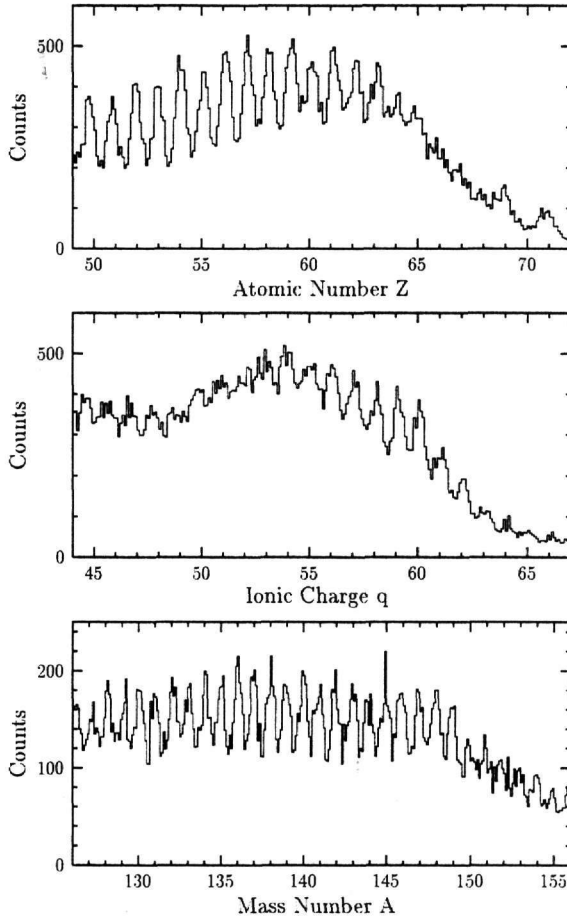


Fig. 1. Typical examples of the Z, q and A spectra of heavy fragments from the reaction of 30 MeV/nucleon  $^{197}\text{Au} + ^{90}\text{Zr}$ .

charge distributions for selected mass values are shown in Fig. 4, where new p-rich nuclei are indicated by larger points.

The position in the Nuclide Chart of the “new” p-rich nuclei observed in this experiment is shown in Fig. 5. By the phrase “new”, we mean these nuclei are not listed in current compilations[16] of nuclear data or recent publications. These nuclei are expected to have short halfives ( $\leq 1$  sec) and some are at or beyond the proton dripline [15]. Use of these hot asymmetric reactions involving massive projectile nu-

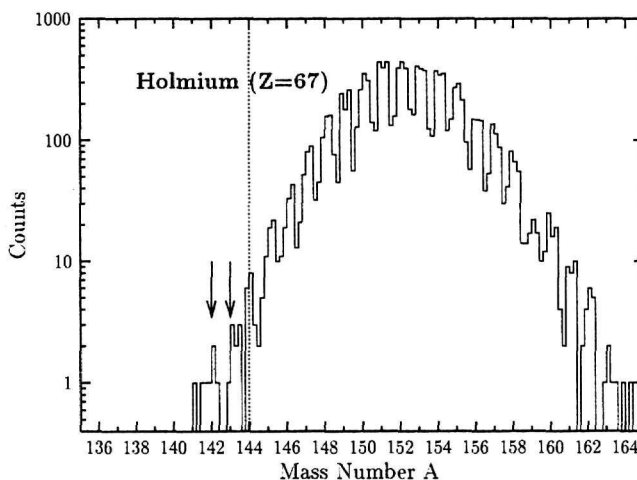


Fig. 2. Mass distribution of holmium ( $Z=67$ ) isotopes from the reaction of 30 MeV/nucleon  $^{197}\text{Au}$  with  $^{90}\text{Zr}$ . The arrows indicate the positions of “new” p-rich nuclei observed in this experiment and the dotted line shows the position of the proton-drip line ( $S_p=0$ ) for this element.

clei seems to complement the more conventional use of symmetric fusion-evaporation nuclear reactions[17] to synthesize and study these proton-rich nuclei. We have arbitrarily defined the “observation” of a “new” nucleus to be the observation of at least 3 counts, which corresponds roughly to a production cross section of  $\sim 40\mu\text{b}$  corresponding to that nucleus.

We have attempted to evaluate whether the production of these “new” nuclei is consistent with the time-of-flight of the particles through the separator ( $\tau \geq 200$  ns). The typical estimated EC halfives of these nuclei [18] are milliseconds or longer. Since several of these nuclei are expected to be proton emitters [16], we calculated the expected proton decay lifetimes for these nuclei using the WKB approximation [19]. We assumed the emitted proton was in the spherical shell model ground state orbital. We assumed a nuclear potential of the Becchetti-Greenlees form [20] with electron screening corrections being calculated using the Huang et al. [21] electron binding energies. The  $Q_p$  values were taken from the mass tables of Liran and Zeldes [14]. In all cases, the calculated halfives were greater than the transit time through the spectrometer.

The typical magnitude of the production cross sections is  $50\text{--}100\mu\text{b}$  which is more than 10 times the typical production cross sections observed in the symmet-

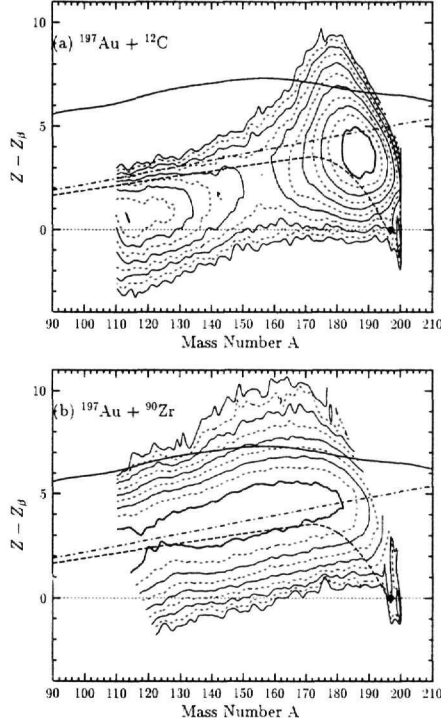


Fig. 3. Fragment yield distributions as a function of  $Z$  (relative to the line of  $\beta$  stability,  $Z_\beta$ ) and  $A$  for the reaction of 30 MeV/nucleon  $^{197}\text{Au}$  with  $^{90}\text{Zr}$ . The dashed line indicates the expected values for relativistic nuclear collisions [12], the dot-dashed line indicates the position of the “evaporation residue attractor line” [13] and the solid line indicates the average position of the proton dripline for odd  $Z$  nuclei [15].

ric compound nuclear reactions usually used to synthesize proton emitting nuclei [17]. It is interesting to evaluate what beam intensities one might expect for the proton-rich nuclei studied in this work if they were produced at a second generation PF facility[22]. Assuming a primary  $^{197}\text{Au}$  beam intensity of 1 particle nA at 30 MeV/nucleon[23], the same production cross sections observed in this work, a production target thickness of 10 mg/cm<sup>2</sup> of  $^{90}\text{Zr}$ , a fragment separator angular acceptance of 10 msr, and a momentum acceptance of 6%, one can estimate secondary beam intensities of these drip-line nuclei of 100 nuclei per hour at 30 MeV/nucleon. Such intensities may enable many new studies of these nuclei.

By studying the proton decay of these exotic nuclei, one can gain unique information about the ordering of the single particle levels and the shell structure of the dripline nuclei[24]. By using the technique described here, one may also be able to produce and study the highly deformed ( $\beta > 0.4$ ) light rare earth nuclei and the position

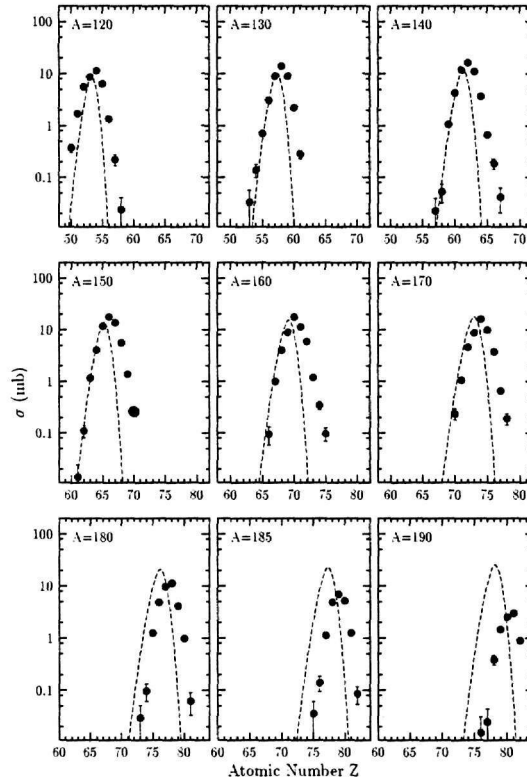


Fig. 4. Fragment charge distributions for selected values of the mass number  $A$  for the reaction of 30 MeV/nucleon  $^{197}\text{Au}$  with  $^{90}\text{Zr}$ . The dashed curves show the expected charge distributions for relativistic nuclear collisions [12]. “New” prich nuclei are indicated with larger symbols.

of the proton drip line in cases where ordinary fusion-evaporation reactions do not yield sufficient numbers of nuclei to study. Studies of di-proton emission in the rare earths (and the heavy nuclei) may be possible[25].

### 3 Production of Neutron-Rich Nuclides by $^{238}\text{U}$ Projectile Fission

The experimental work on the fission of  $^{238}\text{U}$  projectiles was also performed at the National Superconducting Cyclotron Laboratory at Michigan State University using the A1200 (see previous section). The description of the experiment, data analysis procedures and the identification of new n-rich nuclides are reported in Ref. [6] and are in general the same as in the Au fragmentation work. However, a short description of the experimental conditions will be given here.



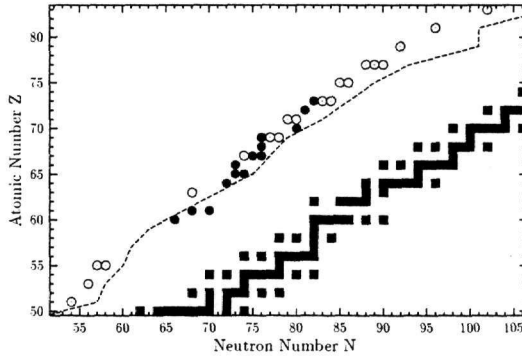


Fig. 5. Z-N plot showing the position of the “new” nuclides observed in this work (solid circles). Open circles represent known proton emitters. Stable nuclei are shown with squares. The dashed line represents the proton-drip line for odd-Z nuclei (from [15]).

A 20 MeV/nucleon  $^{238}\text{U}$  beam ( $i=0.04$  particle nA) struck a production target of  $^{208}\text{Pb}$  ( $5.8 \text{ mg/cm}^2$ , 99.1% enriched) at an angle of  $1^\circ$  relative to the optical axis of the spectrometer. Recoiling fragments from the target, arriving at the first dispersive image of the spectrometer, passed through a slit defining a 3% momentum acceptance and an X-Y position-sensitive parallel-plate avalanche counter (PPAC) also providing a “start” timing signal. At the focal plane (14 m from the start detector), the fragments passed through a microchannel plate timing detector (giving a “stop” signal) and then into a four element (50, 50, 300 and 500  $\mu\text{m}$ ) Si detector telescope. For each event, time-of-flight (resolution 0.8 ns FWHM, typical TOF 240 ns),  $dE/dx$ ,  $E$  and magnetic rigidity ( $B\rho$ ) were recorded. The spectrometer and the detectors were calibrated using low intensity  $^{238}\text{U}$  beam and a series of analog beams ( $^{197}\text{Au}$ ,  $^{156}\text{Gd}$ ,  $^{136}\text{Xe}$ ,  $^{129}\text{Xe}$ ,  $^{109}\text{Ag}$ ,  $^{95}\text{Mo}$ ,  $^{68}\text{Zn}$  and  $^{27}\text{Al}$ ) covering a wide range of  $Z$ ,  $A$  (at three different energies). From the measured quantities and the calibration data, the values of the atomic number  $Z$ , ionic charge  $q$ , mass number  $A$  and velocity were calculated event-by-event. The resolution for  $Z$ ,  $q$  and  $A$  for fragments with mass around  $A=100$  were 0.5, 0.4 and 0.7 units respectively (Fig. 6).

Among the fission fragments of this reaction, a number of “new” n-rich nuclei in the region  $Z=38\text{--}48$  were observed [6]. As an example, the mass distribution of Mo ( $Z=42$ ) fragments is shown in Fig. 7, where two “new” n-rich nuclei are observed (indicated by arrows). However, it should be noted that these nuclei have been reported in the published or unpublished observations of relativistic projectile fission [5]. The present work confirms that finding using a different production mechanism (see below).

The isobaric yield distribution of fission fragments from the reaction of  $^{238}\text{U}$  with  $^{208}\text{Pb}$  is symmetric [6], which rules out any significant contribution of low-energy

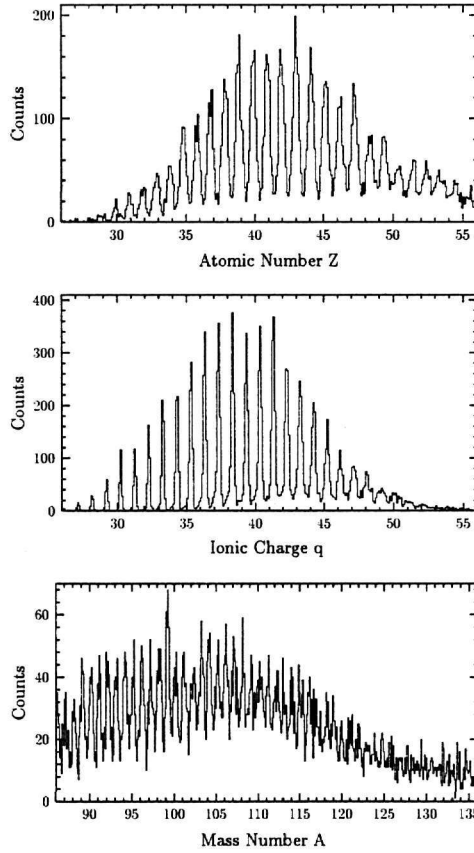


Fig. 6. Typical examples of measured  $Z$ ,  $q$  and  $A$  distributions for fission fragments from the reaction of 20 MeV/nucleon  $^{238}\text{U}$  with  $^{208}\text{Pb}$  at a single spectrometer setting.

fission processes in the reaction mechanism. In addition, the velocity distributions of the reaction products are consistent with a quasielastic (or deep-inelastic) collision of U on the Pb target followed by fission. This statement is supported by a related study of the reaction 24.3 MeV/nucleon  $^{238}\text{U} + ^{197}\text{Au}$  [26].

In Fig. 8, the yield distributions are shown as  $Z$ - $A$  contour plots with  $Z$  given relative to the line of  $\beta$  stability [11]. The fission fragment distributions lie on the neutron-rich side of the stability line. These distributions are compared with the centroids of the C+U products (solid and dashed straight-line segments) [27], with the radiochemical data of  $p(24\text{ MeV}) + ^{238}\text{U}$  [28] (dotted line) and, finally, the centroids of the charge distributions from the n-induced fission of  $^{235}\text{U}$  [29] (solid line). Charge distributions for selected mass values are shown in Fig. 9 and compared with the charge distributions from n-induced fission of  $^{235}\text{U}$  [29] (solid line). Also in this figure are shown the charge distributions of fission fragments from a parallel measurement of the reaction  $^{238}\text{U}$  (20 MeV/nucleon) +  $^{27}\text{Al}$  [6] in which

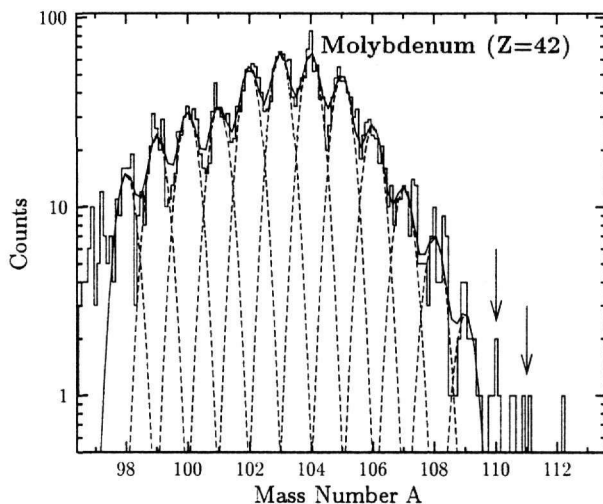


Fig. 7. Mass histogram for the molybdenum ( $Z=42$ ) fragments from the interaction of 20 MeV/nucleon  $^{238}\text{U}$  with  $^{208}\text{Pb}$  with arrows indicating the “new” n-rich nuclei.

the majority of the fission fragments were rather n-deficient [30].

The individual charge distributions for each mass  $A$ , which are very broad (with typical  $\sigma_z \simeq 1.2$ ), were fitted with Gaussian functions. The parameters of these functions were used to estimate the cross sections of (unobserved) very n-rich nuclides that could be produced using the present approach. The results of these calculations are shown in a schematic way in Fig. 10 with open circles of variable size. Stable nuclei are represented by squares. The solid circles are the most n-rich nuclides produced in this experiment. For comparison, a typical path for the astrophysical r-process (dashed line) and the position of the odd- $Z$  neutron drip-line (dotted line) are also shown. These lines are taken from Ref. [15].

It is interesting to evaluate, using these cross section estimates, what rates we might expect for very short-lived n-rich nuclei at a second generation PF facility. For this purpose, we assume a primary  $^{238}\text{U}$  beam intensity of  $5 \times 10^{10}$  [22] at 50 MeV/nucleon, and the same fragment production cross sections and charge distributions as obtained in this work. The higher beam energy will provide substantial forward focussing of the fission fragments. Furthermore, we assume a production target thickness of  $25 \text{ mg/cm}^2$   $^{208}\text{Pb}$ , a fragment separator angular acceptance of 10 msr and momentum acceptance of 6%. Under these conditions, we expect an increase in the production rate by a factor of  $10^5$  as compared with the present experiment and estimate that a production cross section of 1 nb corresponds to a production rate of 10 counts/day.

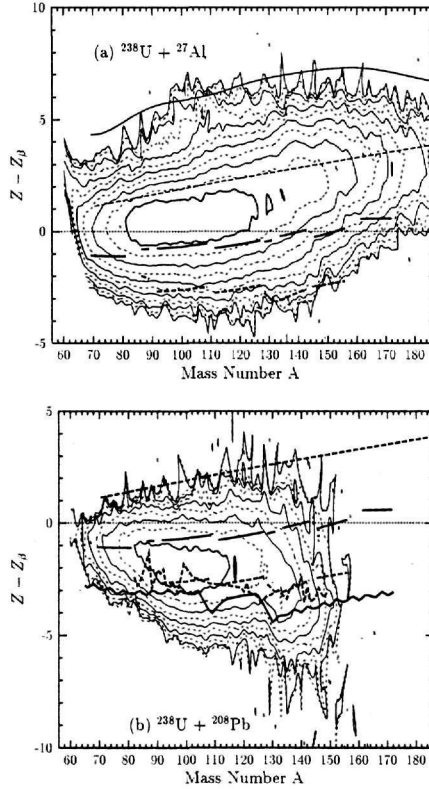


Fig. 8. Fragment yield distributions as a function of  $Z$  (relative to stability), and  $A$  for the 20 MeV/nucleon reaction of  $^{238}\text{U}$  with  $^{208}\text{Pb}$ . Highest yield contours are plotted with thicker lines. Successive contours correspond to a drop of the yield by a factor of 2. The solid-line and dashed-line segments show the values from  $^{12}\text{C}$  (20 MeV/nucleon) +  $^{238}\text{U}$  [27]. The lower dotted line is from  $p$  (24 MeV) +  $^{238}\text{U}$  [28] and the solid line from the  $n$ -induced fission of  $^{235}\text{U}$  [29].

We conclude that for a large number of very  $n$ -rich nuclei, production rates of 10-1000 /sec (at 50 MeV/nucleon) are possible, allowing the study of the structure of these nuclei. For very neutron rich nuclei along the  $r$ -process path, the predicted halflives [31] are less than 1 second, making their production in ISOL facilities very difficult. For such nuclei, counting rates of 10-1000 /day should be reachable which suffices to verify their stability and in the most favorable cases allow measurements of their decay properties. As an example, we can estimate the production cross sections for the  $r$ -process waiting point nuclei  $^{129}\text{Ag}$ ,  $^{128}\text{Pd}$  and  $^{127}\text{Rh}$  ( $N=82$  isobars) to be  $0.5\mu\text{b}$ ,  $50\text{nb}$  and  $0.6\text{nb}$  respectively, and predict counting rates of 4000, 500 and 5 particles/day, respectively. Finally, an interesting observation from Fig. 10, is the possibility to approach the neutron drip-line in the region  $Z=45-50$  ( $A=130-140$ ) with the present approach.

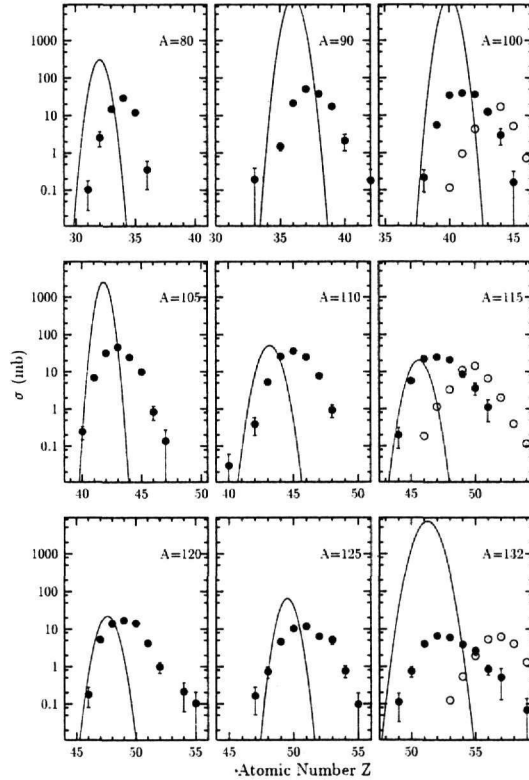


Fig. 9. Charge distributions for representative nuclei formed in the 20 MeV/nucleon  $^{238}\text{U} + ^{208}\text{Pb}$  reaction. Also shown are similar data for thermal neutron induced fission of  $^{235}\text{U}$  (solid lines) and the 20 MeV/nucleon  $^{238}\text{U} + ^{27}\text{Al}$  reaction [6] (open circles).

#### 4 Summary and Conclusions

In summary, the projectile fragmentation of very heavy beams at intermediate energy was presented as a novel way to create and study new heavy nuclei at the limits of nuclear stability. Specifically, intermediate-energy  $^{197}\text{Au}$  fragmentation is shown to be a fruitful avenue for the synthesis of new proton-rich nuclei. Intermediate-energy  $^{238}\text{U}$  projectile fission, on the other hand, leads to the efficient production and separation of extremely neutron rich nuclei.

In the present study, the measured production cross sections indicate that useful intensities of very short-lived proton-rich or neutron-rich nuclei could be produced at intermediate-energy (or possibly lower-energy) PF facilities (which may complement

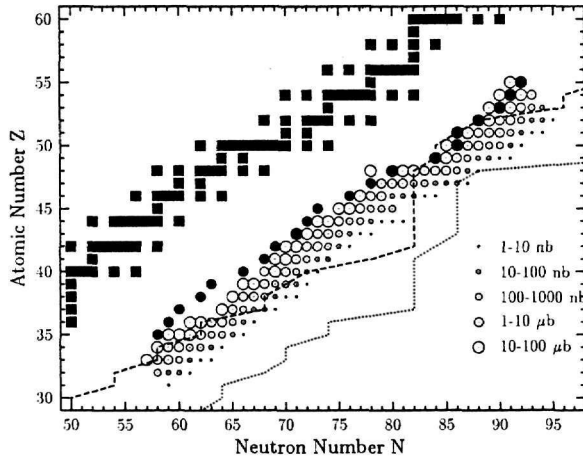


Fig. 10. Z-N plot displaying cross section estimates (open circles) of very neutron-rich nuclei from the interaction of 20 MeV/nucleon  $^{238}\text{U}$  with  $^{208}\text{Pb}$ . Stable nuclei are shown with squares. The solid circles are the most n-rich nuclides produced in the experiment. The dashed line shows a typical r-process path and the dotted-line shows the position of the odd-Z neutron drip-line (lines taken from Ref. [15]).

the more intense beams of longer-lived nuclei produced at ISOL facilities) offering new possibilities for nuclear studies at the limits of nuclear stability.

### Acknowledgements

I wish to thank the following people for their participation in the preparation and realization of the experimental measurements: W. Loveland and K.E. Zyromski (Oregon State University), D. J. Morrissey (Michigan State University), G.J. Wozniak (Lawrence Berkeley Nat. Laboratory) and K. Aleklett (Uppsala University). I also gratefully acknowledge the support of the A1200 group and the operations staff at Michigan State University during these measurements and the support of L. Hart in various stages of the data analysis.

### References

- [1] W. Nazarewicz et al., Nucl. Phys. News, Vol. 6, No 3, (1996), p. 17.
- [2] In the ISOL method, a high energy, high intensity light ion beam strikes a thick

target from which the stopped product nuclei diffuse out and enter an ion source of a mass separator.

- [3] In the PF method, a beam of projectile nuclei is fragmented by passing through a thin foil. The resulting products have high kinetic energies, leave the target and are subjected to mass separation directly without passing through an ion source.
- [4] H. Geissel and G. Munzenberg, *Ann. Rev. Nucl. Part. Sci.* 45 (1995) 163.
- [5] M. Bernas et al., *Phys.Lett. B*331 (1994) 19; M. Bernas et al., *Nucl. Phys. A*616 (1997) 352c.
- [6] G. A. Souliotis et al., *Phys. Rev. C*55 (1997) R2146.
- [7] G. A. Souliotis et al., *Phys. Rev. C* (submitted for publication).
- [8] B. M. Sherrill et al., *Nucl. Instrum. Methods B* 56/57 (1992) 1106.
- [9] K. Hanold et al., *Phys. Rev. C* 52 (1995) 1462.
- [10] G. A. Souliotis et al., *Phys. Rev. C* 57 (1998) 3129.
- [11] G. Friedlander et al., *Nuclear and Radiochemistry*, 3rd Edition (Wiley, New York, 1981) p. 45.
- [12] K. Sümmerer et al., *Phys. Rev. C* 42 (1990) 2546.
- [13] R. J. Charity, *Phys. Rev. C*58 (1998) 1073.
- [14] S. Liran and N. Zeldes, *At. Data and Nucl. Data Tables* 17 (1976) 431.
- [15] P. Moller, J. Nix, and K. Kratz, *At. Data Nucl. Data Tables* 66 (1997) 131.
- [16] See, for example, *Table of Isotopes*, 8th Edition, R. B. Firestone, Ed. (Wiley, New York, 1996), or the more comprehensive ENSDF compilation (as of February, 1999)
- [17] See, for example, C. N. Davids, et al., *Phys. Rev. C*55 (1997) 2255.
- [18] See, for example, M. Hirsch et al., *At. Data Nucl. Data Tables* 53 (1993) 165.
- [19] S. Hofmann, in *Nuclear Decay Modes*, D. N. Poenaru, ed., (Instit. Physics, Bristol, UK, 1996) p. 143.
- [20] F. D. Becchetti and G. W. Greenlees, *Phys. Rev.* 182 (1969) 1190.
- [21] K. N. Huang and H. Mark, *At. Data and Nucl. Data Tables* 18 (1976) 243.
- [22] The K500 $\otimes$ K1200 Proposal, MSUCL-939, 1994.
- [23] Marti, F., private communication.
- [24] S. Aberg, P. B. Semmes and W. Nazarewicz, *Phys. Rev. C*56 (1997) 1762.
- [25] European Radioactive Beam Facilities, NUPECC, May 1993.

- [26] E. Piasecki et al., Phys. Lett. B 351 (1995) 412.
- [27] C.H. Lee et al., Phys. Rev. C38 (1988) 1757.
- [28] H. Kudo et al., Phys. Rev. C57 (1998) 178.
- [29] A.C. Wahl, At. Data Nucl. Data Tables 39 (1988) 1.
- [30] G. A. Souliotis et al., in preparation.
- [31] A. Staudt et al., At. Data N. Data Tables 44 (1990) 79.

j.